Egypt. J. Chem. **Vol. 69**, No. 3 pp. 1 - 7 (2026)

Egyptian Journal of Chemistry

http://ejchem.journals.ekb.eg/

Synthesis, Characterization and Frequency-Dependent Dielectric Applications of New Indole–Oxindole-Based on Propanenitrile Derivatives

Hemat S. Khalaf [1,*], Tarek B. A. El-Naggar [2], Ragab M. Mahani[3], Elshahat H.A. Nashy[4], Ahmed H. Shamroukh [1,*]

[1]*Photochemistry Department, Chemical Industries Research Institute, National Research Centre, 33 El Buhouth Street, P.O. Box 12622, Cairo, Egypt*

[2]*Department of Chemistry of Natural and Microbial Products, Pharmaceutical and Drug Industries Research Institute, National Research Centre, 33 El Buhouth Street, P.O. Box 12622, Cairo, Egypt.*

[3]*Physics and Dielectrics Dept., Physics Research Institute, National Research Centre, 33 El Buhouth Street, P.O. Box 12622, Cairo, Egypt*

[4]*Chemistry of Tanning Materials Dept., Chemical Industries Research Institute, National Research Centre, 33 El Buhouth Street, P.O. Box 12622, Cairo, Egypt*

Abstract

In the current study, a new series of 3-(1H-indol-3-yl)-3-oxo-2-(2-oxoindolin-3-ylidene) propanenitrile derivatives **3a-d** were prepared from condensation of 3-indolyl-3-oxopropanenitrile (1) with isatin derivatives **2a-d** in the presence of piperidine as a catalyst. Compounds 3a-d was characterized using spectroscopic techniques and elemental analysis (CHNS). The dielectric properties like the permittivity (ε'), loss tangent ($tan\delta$), and electric modulus (M' and M'') were evaluated over a wide frequency range (0.1 Hz–10 MHz) to understand energy storage, energy loss, and relaxation processes in organic compounds **3a-d**. Compounds **3a-c** show higher permittivity values at low frequencies due to the contribution of dipolar and interfacial polarization. Compound **3b** exhibits the strongest polarization and highest energy loss at low frequencies, likely influenced by its methyl group. Compound **3c** exhibits moderate dielectric properties arising from the electron-withdrawing chloro group. Compound 3d shows constant ε' and very low $tan\delta$ throughout the entire frequency range, indicating weak or absent dipolar relaxation, likely caused by its rigid benzyl substituent. Electric loss modulus (M'') analysis confirms these findings, showing clear relaxation peaks in compounds **3a-c** and no significant peak for compound **3d**. Interestingly, the observed relative low permittivity and very loss values measured at high frequencies (10 MHz) make compounds **3b-d** promising for high-speed signal transmission with minimal attenuation.

Keywords: Indole, Oxindole, Propanenitrile Derivatives, Permittivity, Loss tangent.

1. Introduction

Traditionally, electrical conductivity has been associated with inorganic materials such as metals and semiconductors [1]. However, over the past few decades, a new class of organic conducting materials has emerged, revolutionizing the field of materials science. These are carbon-based compounds that can conduct electricity, offering a lightweight, flexible, and potentially low-cost alternative to traditional conductors [2]. Organic conducting materials are primarily composed of conjugated polymers or small molecules containing alternating single and double bonds. This π-conjugation allows for the delocalization of electrons across the molecular backbone, enabling charge transport when the material is appropriately doped (chemically modified to introduce charge carriers) [3]. These materials can exhibit semiconducting or even metallic levels of conductivity and are being extensively studied for applications in flexible electronics [4], organic solar cells (OPVs) [5], organic light-emitting diodes (OLEDs) [6], biosensors [7] and wearable technology [8]. The appeal of conducting organic materials lies not only in their electrical properties but also in their mechanical flexibility, tunable electronic structure, and solution-processability, making them ideal for printable electronics and next-generation device fabrication [9]. Organic compounds can also include other heteroatoms like nitrogen and oxygen. They can behave differently when exposed to an electric field, exhibiting a wide range of dielectric behaviors and properties. Their dielectric properties originate from the polarizability of the constituent molecules, molecular structure, and functional groups. The dielectric properties include permittivity (ε'), dielectric loss (ε''), and loss tangent ($tan\delta$), describe how the material responds to an alternating or AC

*Corresponding author e-mail: hematsalama2016@gmail.com (Hemat S. Khalaf); ahshamroukh@yahoo.com (Ahmed H. Shamroukh).

Received date 28 September 2025; Revised date 13 November 2025; Accepted date 23 November 2025

DOI: 10.21608/ejchem.2025.427898.12400

electric field. Many organic compounds have a "polar" nature, meaning they can orient or polarize when an electric field is applied. Interfacial or space charge polarization may dominate the dielectric properties of heterogeneous systems or composite structures. The response of organic material to an electric field is frequency and temperature-dependent, with relaxation processes corresponding to molecular motions such as dipole reorientation. Organic materials have been widely used in various applications because of their flexibility, tunable chemical structure, processability, and cost-effectiveness. Their applications range from capacitors (which store electricity), insulators (which keep electricity from escaping), sensors (which detect changes), and even in electronics. Understanding how these materials respond to an electric field helps scientists and engineers improve the products performance and quality. Indole is a core structure found in many natural and synthetic organic compounds, and its derivatives are known for their diverse pharmacological effects [10-12]. Indole is not intrinsically conductive; however, it can be polymerized to form polyindole (PIn), a conducting polymer with promising applications across multiple fields. Polyindole exhibits advantageous properties such as low toxicity, good environmental stability, and notable redox activity. These characteristics make PIn a strong candidate for use in electronics, battery anode materials, electrocatalysis, and pharmaceutical applications [13]. The present study focuses on the synthesis of 3-(1H-indol-3-yl)-3-oxo-2-(2-oxoindolin-3-ylidene)propanenitrile derivatives, combining indole and oxindole moieties within a single conjugated π-system. This extended delocalization, spanning the indole, oxindole, α,β-unsaturated carbonyl, and nitrile groups, facilitates efficient π-electron flow-an essential feature in organic semiconductors and electronic materials. Additionally, the incorporation of electron-donating (indole) and electron-withdrawing (cyano, carbonyl) groups creates a push–pull electronic system, promoting intramolecular charge transfer and enhancing optoelectronic properties. These structural characteristics make the target compounds promising candidates for use in organic semiconductors, electrochromic devices, hole-transporting layers, and chemical sensors. Although limited research has been published on this compound and its derivatives, structurally related molecules have demonstrated nonlinear optical properties and potential applications in organic semiconductor technologies [13-16]. Therefore, to understand more about how this compound and its derivatives work, we investigated their structure as well as their electrical properties (permittivity, loss tangent, and electric modulus formalism) over a wide frequency range (0.1 Hz-10 MHz) at room temperature. This would help to understand how molecular structure of this compound affects its electrical behavior.

2. Results and Discussion

2.1. Chemistry

3-(1*H*-Indol-3-yl)-3-oxo-2-(2-oxoindolin-3-ylidene)propanenitrile derivatives **3a-d** were produced via condensation reaction of 3-indolyl-3-oxopropanenitrile (**1**) and isatin derivatives 2a-d in ethanol using piperidine as a catalyst. The novel derivatives were investigated utilizing spectroscopic techniques (IR, ^{1}H, and ^{13}C NMR) as well as elemental analysis, (scheme1).

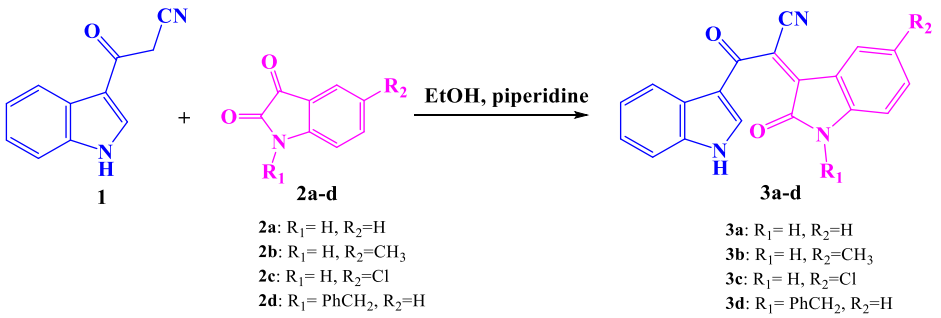

Scheme 1: Synthetic pathway of 3-(1*H*-indol-3-yl)-3-oxo-2-(2-oxoindolin-3-ylidene) propanenitrile derivatives 3a-d.

2.2. Dielectric study

The permittivity (ε′) is one of the key parameters that measures the material's ability to store electrical energy in an electric field [17]. It is a function of electrical capacitance (C) and given as:

$$\varepsilon'(\omega) = C(\omega)\frac{d}{\varepsilon_o A} \qquad (1)$$

where ω is the angular frequency (= 2πf) and f is the applied field frequency in Hertz, ε_o = 8.85×10^{-12} F/m is the permittivity of vacuum, *d* is the sample thickness, *A* is the sample surface area. Figure 1 shows variation of ε' within a wide frequency range (0.1 Hz-10 MHz) for compounds **3a-c** compared to compound **3d**. At low frequencies, compounds **3a-c** show higher permittivity values (~35–55), attributing to various polarization mechanisms, i.e. strong dipolar or/and interfacial polarization [18]. These mechanisms become more mobile and respond well to low-frequency fields. The compound 3b with the highest values (~55), displays the strongest low-frequency polarization, but it also loses dielectric strength rapidly, confirming the

contribution of dipolar polarization. Accordingly, structural features of compound **3b** may enhance charge delocalization or dipole mobility. The relative reduction of permittivity (~35) for compound **3c** suggests a reduction of polarizability due to the chloro-substituent that lowers mobility of dipoles. Based on the above discussion, the relative high permittivity values for these organic compounds **3a-c** indicates their ability to store electric energy in an electric field, thus they can be useful in low-frequency applications, i.e. capacitors, supercapacitors, batteries, etc.

Generally, as the frequency increases, the permittivity (ε') of compounds 3a-c decreases, showing a dielectric dispersion as some polarization mechanisms begin to lag behind the applied electric field. Meanwhile, at higher frequencies, dipoles and space charges cannot follow up the fast changes in electric field [19]. Then, ε' saturates at higher frequencies, suggesting that only intrinsic or fast polarization mechanisms (electronic, ionic) remain active. On the other hand, the permittivity (ε') of 3d saturates at much lower values (~5) and remains almost constant throughout the entire frequency range. Further, it does not show any dielectric dispersion, meaning this compound shows very weak orientation polarization or the present polar entities are rigidly held and cannot respond to the applied field. This is likely because of a bulkier benzyl group, causing steric hindrance and limiting dipole reorientation. In conclusion, the compound **3d** is showing minimal dielectric response compared to the other compounds, with frequency - independent behavior. Based on our previous work [13] the permittivity of compound **3b** either remains constant or continues decrease with increasing frequency and reaches much smaller values within a microwave frequency range (300 MHz-300 GHz). Therefore, this compound would be applicable for high-speed signal transmission with minimum attenuation. To ensure this applicability, low delay characteristics examined by studying the frequency–dependent loss tangent (*tanδ*) of all compounds with focusing our attention to the data reported for compound 3d. Since, *tanδ* measures the electric energy lost by the material as heat or/and leakage current.

The variation of *tanδ* with frequency is illustrated in Figure 2 and Table 1. In general, *tanδ* shows high values at low frequency then decreases as the frequency increases, indicating that the ability of material to dissipate electrical energy becomes less significant as the frequency increases. For compound **3a**, *tanδ* is ~1 at 0.1 Hz, then decreases gradually as the frequency increases. At frequencies above 10^4 Hz, it drops to ~0.01. When we check compound 3b at the lowest frequency value, i.e. 0.1 Hz, *tanδ* is almost 10, which drops quickly as the frequency increases. As a result, compound 3b has the highest *tanδ* value compared to all the other compounds we investigated, meaning it loses a lot of energy probably because of high dipolar relaxation or interfacial polarization. However, at higher frequencies, like in the MHz range, those energy losses become much smaller. For compound 3c, *tanδ* begins just below 0.65 at 0.1 Hz, then decreases steadily in a similar trend to 3b, but the starting value is lower (~0.62). Then, it drops slightly with increasing frequency up to 103 Hz that followed by a significant decrease at higher frequencies, exploring much lower values (~0.013) at 10 MHz. As a result, compound **3c** has moderate loss tangent, less than compound **3b** but more than compound **3a**.

Compared to all the other compounds, compound **3d** exhibits the lowest *tanδ* values throughout the frequency range. It starts around 0.03 at low frequencies and continues to decrease as the frequency increases, showing much lower values (0.0007) at 10 MHz. Interestingly, compound **3d** has very low loss tangent or minimal energy dissipation, making it the least lossy material among the four compounds studied.

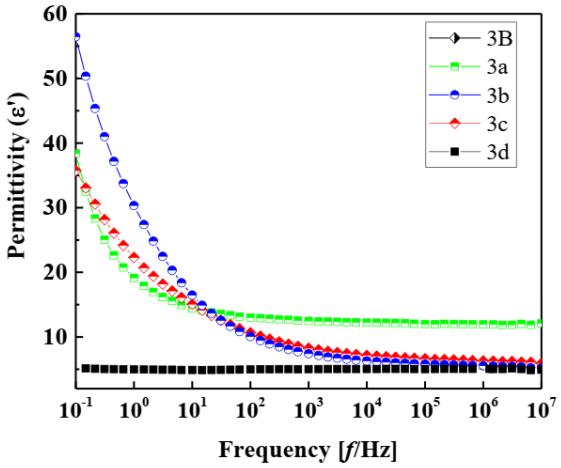

Figure 1: The frequency dependence of permittivity (ε') of compounds 3a–d.

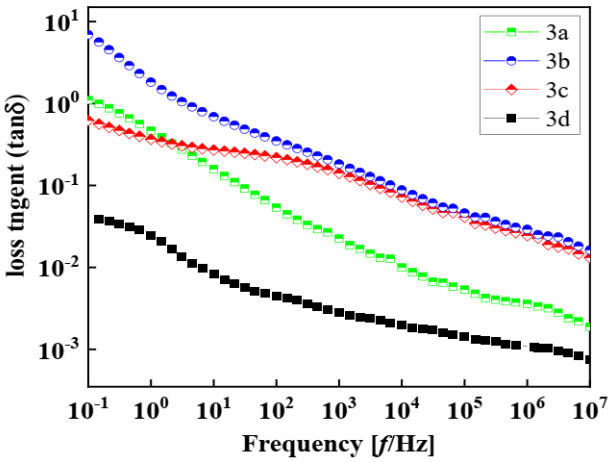

Figure 2: The frequency dependence of loss tangent (*tanδ*) of compounds 3a-d.

Table 1: The permittivity (*ε′*) and loss tangent (*tanδ*) of 3a-d compounds at different frequencies

Compound	Substituent	*ε′*		*tanδ*	
		f = 0.1 Hz	*f* = 10 MHz	*f* = 0.1 Hz	*f* = 10 MHz
3a	None	38	12	1.02	0.002
3b	Methyl	55	5.22	7	0.016
3c	Chloro	35	6	0.62	0.013
3d	Benzyl	5	5	0.04	0.0007

To evaluate the dielectric relaxation behavior of the prepared compounds, the real (*M′*) and imaginary (*M″*) parts of the complex electric modulus (*M**), are analyzed. The electric modulus formalism in terms the permittivity (*ε′*) and dielectric loss (*ε″*= *ε′*×*tanδ*) [20] is defined as:

$$M^*(\omega) = \frac{1}{\varepsilon^*(\omega)} = M' + iM'' = \frac{\varepsilon'}{\varepsilon'^2 + \varepsilon''^2} + i\frac{\varepsilon''}{\varepsilon'^2 + \varepsilon''^2} \qquad (2)$$

This formalism offers insights into the dielectric response while minimizing electrode polarization effect. Here, *M′* represents the ability of material to store electrical energy, whereas *M″* reveals the energy dissipation due to relaxation processes. Figure 3a,b shows the frequency dependence of *M′* and *M″* at ~30°C for the organic compounds **3a-d**. For compounds **3a-c**, *M′* increases with increasing frequency and saturates beyond ~10^3–10^4 Hz, indicating a transition from long-range to short-range ionic mobility accompanied by a reduction in interfacial polarization effects. The elevated values of *M′* at high frequencies related to relaxation processes [21]. The extended tail observed at lower frequencies indicates a significant capacitance associated with the electrodes, supporting the notion of non-Debye behavior. Compound 3b shows the steepest increase in *M′* and reaches the highest values at high frequencies, suggesting enhanced dipolar polarization due to the electron-donating methyl substituent on the isatin part of the molecule that promotes local molecular flexibility and polarizability. Compound 3c has a chloro group that pulls electrons towards it that exhibits a more moderate rise in *M′*. This suggests some restriction in mobility of dipoles and thus the particles move a bit slower than in case of compound **3b**. The unsubstituted compound **3a** exhibits intermediate behavior. In contrast, compound **3d**, containing a bulky benzyl substituent, shows an almost constant M′ response throughout the entire frequency range, indicating minimal dipolar contribution and high structural rigidity. This suggests the greatest ability of compound **3a** to store electric energy compared to other four compounds.

The imaginary part of electric modulus (*M″*) provides valuable information about the dielectric relaxation mechanisms. Compounds **3a-c** show a clear relaxation peak at low frequencies in *M″* spectra (Figure 3b) whereas compound **3d** does not. These peaks originate either from localized dipolar reorientations or interfacial polarization effects. Further, the area under this peak defines a region where charge carriers are constrained to potential wells and can only travel short distances while the peak position identifies the relaxation time (*τ*) of ions in the system. Compound **3b** exhibits the most pronounced, sharp and intense relaxation peak compared to other compounds whose maximum positioned at ~10^2 Hz. These

features indicate the presence of a strong and relatively narrow dielectric relaxation process. In addition, they reflect enhanced dielectric loss due to the methyl substitution that facilitates dipole reorientation and increases segmental mobility upon application of electric field. Compound 3c displays a broader and less intense relaxation peak, suggesting a distribution of different relaxation times for superposition of different polarization mechanisms like interfacial and dipolar polarization. For such a case, the chlorinated derivative may introduce localized electronic effects that may hinder the polarization mechanisms, giving rise a broad relaxation process. Compound **3a** exhibits a sharper and lower-intensity relaxation peak, exploring moderate dielectric relaxation behavior in the absence of electron-donating or -withdrawing substituents. From Figures 3a,b, the observed trends in M'' spectra are consistent with tanδ behavior, which directly proportional to energy dissipation. So, the higher intense M'' peak, the greater the loss tangent ($tan\delta$). Thus, compound 3b exhibits the highest loss, followed by compound **3c** and compound **3a** (see Table 1). In contrast, compound **3d** shows a continuous decrease in M'' with increasing frequency and no recognizable relaxation peak, indicating the absence of any significant dipolar polarization in the studied frequency window. The rigid benzyl substituent may hinder the dipolar motion, making compound **3d** behave more like an insulating material with minimal energy dissipation.

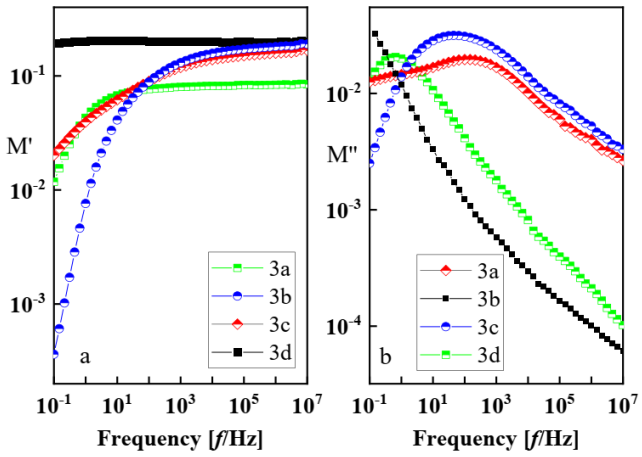

Figure 3: The frequency dependence of the real, M' (a) and imaginary, M'' (b), part of the complex electric modulus (M^*) for compounds 3a-d at ~ 30°C.

Based on the above discussion, compound **3d,** in addition to compound **3b**, and compound **3c** with minimal energy dissipation and relatively low permittivity values at 10 MHz would be promising for high-frequency applications, particularly in high-speed signal transmission with minimum attenuation according to the following relationships [21-23]:
- The relationship between the high - frequency signal propagation speed, V (m/s), and permittivity (ε') is:

$$V = \frac{kc}{\sqrt{\varepsilon'}} \qquad (3)$$

where, k is a constant and c (m/s) is the light speed in a vacuum. This relationship suggests that the lower ε' is, the faster the signal propagation speed will be.
- The relationship between the high - frequency attenuation of signal propagation (α) and loss tangent ($tan\delta$) is:

$$\alpha = k' f tan\delta \sqrt{\varepsilon'} \qquad (4)$$

where α is attenuation of signal propagation or attenuation constant (typically in Np/m or dB/m), k' is a proportionality constant, depends on the unit system used, f is the frequency of signal in Hz.

3. Materials and methods

3.1. Materials and instrumentations

All chemicals purchased from Sigma-Aldrich were used as obtained without further purification. TLC (thin-layer chromatography) was used to monitor chemical reactions using eluent (Petroleum ether: ethyl acetate, 8:2). For TLC, Silica gel 60 F 254 was applied to aluminum sheets (20 X 20 cm). Purification of the products was performed under flash conditions using a column chromatography (Silica gel 60, 0.040–0.063 mm). Shimadzu IR 8400s Spectrophotometer was used to measure FT-IR spectra (ν max in cm−1, KBr). 1H and 13C NMR spectra were recorded on a Bruker High-Performance Digital FT NMR spectrometer, Avance III (400 MHz for 1H and 100 MHz for 13C NMR). ^{1}H and ^{13}C NMR signals were

referenced to tetramethylsilane (TMS) and the solvent shifts of DMSO-d_6. The abbreviations for reporting 1H NMR data were denoted as follows: s, singlet; d, doublet; t, triplet; m, multiplet. Values of the coupling constant (J) were recorded in Hertz (Hz). Electron impact mass spectra were measured using a DI Analysis Shimadzu QP-2010 plus (70 eV). An Elemental Analyzer CHNS-932 (LECO) was used for elemental analyses. The dielectric properties of the prepared organic compounds were carried out over a wide frequency range (0.1 Hz -10 MHz) within a temperature range at 30^{o}C using a broadband dielectric spectrometer (BDS), Concept 40, Novo Control, Germany.

3.2. General Procedure for the preparation of derivatives 3a-c:
A mixture of an equimolar amount of 3-indolyl-3-oxopropanenitrile (1) [24,25] and isatin derivatives 2a-c in absolute ethanol (20 mL) in the presence of piperidine as a catalyst was heated at 80 ^{o} C for 5-12 h (the reaction progress was monitored by TLC). Upon completion, the reaction mixture was cooled to room temperature. The formed product was filtered, dried and purified using a column chromatography (Silica gel 60, 0.040–0.063 mm) to afford compounds 3a-d.

3-(1*H*-indol-3-yl)-3-oxo-2-(2-oxoindolin-3-ylidene) propanenitrile (3a)
white powder; (Yield 86 %); m.p., 215-216 ^{o} C; IR (KBr) ν cm-1: 3378 (NH), 3348 (NH), 3027 (aromatic H), 2228 (C≡N), 1735 (C=O), 1670 (C=O); ^{1}H NMR (DMSO-d_6) δ ppm: 7.10-7.37 (m, 7H, Ar-H), 8.29 (d, 1H, Ar-H), 8.46 (s, 1H, pyrrole-H), 11.29 (s, 1H, NH, D_2O exchangeable), 11.94 (s, 1H, NH, D_2O exchangeable); 13C NMR (DMSO-d_6) δ ppm: 113.02 (CN), 122.46-137.02 (C_{Ar}), 171.15 (C=O), 181.97 (C=O); MS, m/z (%): 313.12 (M+, 81); Anal. Calcd. For $C_{19}H_{11}N_3O_2$ (313.09) (%): C, 72.84; H, 3.54; N, 13.41. Found (%): C, 72.77; H, 3.59; N, 13.37.

3-(1*H*-indol-3-yl)-2-(5-methyl-2-oxoindolin-3-ylidene)-3-oxopropanenitrile (3b)
white powder; (Yield 74 %); m.p., 228-230 ^{o} C; IR (KBr) ν cm-1: 3375 (NH), 3350 (NH), 3022 (aromatic H), 2217 (C≡N), 1738 (C=O), 1677 (C=O); ^{1}H NMR (DMSO-d_6) δ ppm: 2.26 (s, 3H, CH_3), 6.92-7.63 (m, 7H, Ar-H), 8.31 (d, 1H, Ar-H), 8.40 (s, 1H, pyrrole-H), 11.11 (s, 1H, NH, D_2O exchangeable), 11.91 (s, 1H, NH, D_2O exchangeable); ^{13}C NMR (DMSO-d_6) δ ppm: 21.82 (CH_3), 113.12 (CN), 121.37-139.15 (C_{Ar}), 171.13 (C=O), 181.95 (C=O); MS, m/z (%): 327.34 (M+, 76); Anal. Calcd. For $C_{20}H_{13}N_3O_2$ (327.10) (%): C, 73.38; H, 4.00; N, 12.84. Found (%): C, 73.46; H, 3.96; N, 12.79.

2-(5-chloro-2-oxoindolin-3-ylidene)-3-(1*H*-indol-3-yl)-3-oxopropanenitrile(3c)
white powder; (Yield 89 %); m.p. 210-211 ^{o} C; IR (KBr) ν cm-1: 3388 (NH), 3372 (NH), 3089 (aromatic H), 2222 (C≡N), 1725 (C=O), 1669 (C=O); ^{1}H NMR (DMSO-d6) δ ppm: 7.27-7.76 (m, 7H, Ar-H), 8.31 (d, 1H, Ar-H), 8.47 (s, 1H, pyrrole-H), 11.24 (s, 1H, NH, D_2O exchangeable), 12.64 (s, 1H, NH, D_2O exchangeable); ^{13}C NMR (DMSO-d_6) δ ppm: 113.18 (CN), 122.17-138.95 (C_{Ar}), 169.97 (C=O), 182.03 (C=O); MS, m/z (%): 349.00 (M+, 24). 347.45 (M+, 72); Anal. Calcd. For $C_{19}H_{10}ClN_3O_2$ (347.05) (%): C, 65.62; H, 2.90; Cl, 10.19; N, 12.08. Found (%): C, 65.70; H, 2.84; Cl, 10.14; N, 12.13.

2-(1-benzyl-2-oxoindolin-3-ylidene)-3-(1*H*-indol-3-yl)-3-oxopropanenitrile (3d)
white powder; (Yield 77 %); m.p. 220-222 ^{o} C; IR (KBr) ν cm-1: 3375 (NH), 3090 (aromatic H), 2221 (C≡N), 1728 (C=O), 1670 (C=O); ^{1}H NMR (DMSO-d_6) δ ppm: 3.18 (s, 2H, CH_2), 7.04-7.53 (m, 10H, Ar-H), 8.21-8.23 (m, 3H, Ar-H), 8.52 (s, 1H, pyrrole-H), 12.45 (s, 1H, NH, D_2O exchangeable); ^{13}C NMR (DMSO-d_6) δ ppm: 47.37 (CH_2), 113.29 (CN), 122.37-147.38 (C_{Ar}), 169.19 (C=O), 182.11 (C=O). MS, m/z (%): 403.13 (M+, 75); Anal. Calcd. For $C_{26}H_{17}N_3O_2$ (403.44) (%): C, 77.41; H, 4.25; N, 10.42. Found (%): C, 77.35; H, 4.31; N, 10.38.

3. Conclusions
A series of 3-(1H-indol-3-yl)-3-oxo-2-(2-oxoindolin-3-ylidene) propanenitrile derivatives **3a–d** was synthesized and characterized using various spectroscopic techniques. The dielectric behavior of the compounds was found to be highly dependent on both frequency and molecular structure. Compounds **3a–c** exhibited relatively high permittivity values at low frequencies, indicating enhanced energy storage capabilities due to dipolar and interfacial polarization effects. Notably, compound 3b displayed the highest energy storage capacity and significant energy loss at low frequencies. In contrast, compound 3c showed reduced permittivity and moderate loss, presumably due to the dipole-restricting effect of the chloro substituent. At higher frequencies (~10 MHz), all compounds exhibited a marked decrease in both permittivity and loss tangent, with compound 3d showing the most pronounced decline. Interestingly, compound **3d** exhibited no dielectric dispersion or relaxation peaks within the studied frequency range, suggesting minimal polarization activity. This behavior is likely due to the bulky benzyl group, which restricts dipole mobility. Consequently, compound **3d** recorded the lowest permittivity (~5) and loss tangent (0.0007) values at 10 MHz. These low values render compounds **3b–d** particularly promising for high-speed signal transmission applications, where minimal attenuation is required. The combination of low permittivity, low dielectric loss, and cost-effective synthesis makes these compounds attractive candidates for advanced electronic and dielectric applications.

4. Conflicts of interest
The authors declare no conflict of interest.

5. References
[1] R. Levy, A. Katchalsky, Electrical conductivity of sodium and calcium forms of the synthetic inorganic exchanger zeolite type A. Journal of Colloid and Interface Science, 1973,42, 366-371, https://doi.org/10.1016/0021-9797(73)90301-9.

[2] M. Koopmans, M. A. T. Leiviskä, J. Liu, J. Dong, L. Qiu, J. C. Hummelen, G. Portale, M. C. Heiber, L. J. A. Koster, Electrical Conductivity of Doped Organic Semiconductors Limited by Carrier–Carrier Interactions. ACS Applied Materials & Interfaces, 2020, 12, 56222-56230, https://doi.org/10.1021/acsami.0c15490.
[3] H. S. Khalaf, M. A. El-Manawaty, E. R. Kotb, M.T. Abdelrahman, A. H. Shamroukh, Reactivity of 2-((3-Cyano-4-(4-Fluorophenyl)-6-(Naphthalen-2-yl)Pyridin-2-yl)Oxy)Acetohydrazide Toward Some Reagents for Preparing a Promising Anticancer Agents and Molecular Docking Study. Chemistry & Biodiversity, 2025, 22, e202403463. https://doi.org/10.1002/cbdv.202403463.
[4] H. S. Khalaf, E. R. Kotb, N. A. M. Abdelwahed, M. T. Abdelrahman, A. H. Shamroukh, Reactivity of (3-(4-Fluorophenyl)oxyran-2-yl)(naphthalene-2-yl)methanone Toward Some Nucleophiles for Preparing Promising Agents with Antimicrobial and Antioxidant Activities, Chemistry Select, 2024, 9, e202404371, https://doi.org/10.1002/10.1002/slct.202404371.
[5] B. P. Dash, S. K. Beriha, B. Naik, P. K. Sahoo, Organic materials based solar cells. Materials Today: Proceedings, 2022, 67, 1057-1063, https://doi.org/10.1016/j.matpr.2022.07.002.
[6] Z. B. Wang, M. G. Helander, Z. H. Lu, 2-Transparent conducting thin films for OLEDs, Editor(s): Alastair Buckley, In Woodhead Publishing Series in Electronic and Optical Materials. Organic Light-Emitting Diodes (OLEDs), Woodhead Publishing, 2013, 49-76, https://doi.org/10.1533/9780857098948.1.49.
[7] J. B. Kaushal, P. Raut, S. Kumar, Organic Electronics in Biosensing: A Promising Frontier for Medical and Environmental Applications. Biosensors, 2023, 13, 976. https://doi.org/10.3390/bios13110976.
[8] R. Xiao, X. Zhou, C. Zhang, X. Liu, S. Han, C. Che, Organic Thermoelectric Materials for Wearable Electronic Devices. Sensors, 2024, 24, 4600. https://doi.org/10.3390/s24144600
[9] K. Namsheer, C. S. Rout, Conducting polymers: a comprehensive review on recent advances in synthesis, properties and applications. RSC Advances, 2021, 11, 5659-5697. https://doi.org/10.1039/d0ra07800j.
[10] H. S. Khalaf, M. S. Abdel-Aziz, M. A. A. Radwan, A. A. Sediek, Synthesis, Biological Evaluation, and Molecular Docking Studies of Indole-Based Heterocyclic Scaffolds as Potential Antibacterial Agents, Chemistry & Biodiversity, 2024, e202402325, https://doi.org/10.1002/cbdv.202402325
[11] H. S. Khalaf, A. A. Abd El-Gwaad, A. F. El-Sayed, H. M. Awad, A. A. Fayed, Synthesis, Molecular Docking, and Pharmacological Evaluations of Novel Pyrimidine Derivatives Chemistry & Biodiversity (2025): 22:e202500477. https://doi.org/10.1002/cbdv.202500477.
[12] N. A. Hamdy, H.S. Khalaf, M. M. Mounier, M. K. El-Ashrey, M. M. Anwar, Discovery of novel tetralin-thiazole conjugates as VEGFR-2 inhibitors with anticancer potential: an integrated computational and biological study, Journal of Molecular Structure 1349 (2026): 143602. https://doi.org/10.1016/j.molstruc.2025.143602
[13] J. Arjomandi, D. Nematollahi, A. Amani, Enhanced Electrical Conductivity of Polyindole Prepared by Electrochemical Polymerization of Indole in Ionic Liquids J. Appl. Polym. Sci. 131, 40094, https://doi.org/10.1002/app.40094
[14] S. Kumar, A. Ritika, brief review of the biological potential of indole derivatives. Future Journal of Pharmaceutical Sciences, 2020, 6, 121. https://doi.org/10.1186/s43094-020-00141-y.
[15] M. Koopmans, M. A. T. Leiviska, J. Liu, J. Dong, L. Qiu, J. C. Hummelen, G. Portale, M. C. Heiber, L. J. A. Koster, Electrical Conductivity of Doped Organic Semiconductors Limited by Carrier−Carrier Interactions. ACS Applied Material Interfaces, 2020, 12, 56222−56230. https://dx.doi.org/10.1021/acsami.0c15490.
[16] R.-Y. Yang, M.-H. Weng, C.-Y. Hung, H.-W. Wu, Y.-K. Su, Loss characteristics of silicon substrate with different resistivities. Microwave and optical technology letters, 2006, 48, 1773-1776. https://doi.org/10.1002/mop.21786
[17] L. D. Landau, E. M. Lifshitz, L. P. Pitaevskii, Electrodynamics of continuous media, Elsevier Butterworth-Heinemann. 2009, ISBN 978-0-7506-2634-7. OCLC 756385298.
[18] J. C. Maxwell, A Treatise on Electricity and Magnetism. Oxford University Press. Original theoretical background for interfacial polarization (Maxwell–Wagner polarization), 1892.
[19] S. S. Du, X. F. Luo, J. X. An, Z. J. Zhang, S. Y. Zhang, Y. R. Wang, Y. Y. Ding, W. Q. Jiang, B. Q. Zhang, Y. Ma, Y. Zhou, Y. M. Hu, Y. Q. Liu. Exploring boron applications in modern agriculture: Antifungal activities and mechanisms of phenylboronic acid derivatives. Pest Management Science, 2023, 79, 2748-2761.
[20] A. El Hachmi, B. Manoun, Complex dielectric, electric modulus, impedance, and optical conductivity of Sr3-x-PbxFe2TeO9 (x =1.50, 1.88 and 2.17). International Journal Materials Research, 2023, 114, 100–110. https://doi.org/10.1515/ijmr-2022-0189.
[21] K. Karoui, A. B. Rhaiem, F. Jemni, Li2M(WO4)2 (M = Ni, Cu, Co): electrical, thermal, and optical properties. Ionics, 2021, 27, 1511–1524. https://doi.org/10.1007/s11581-021-03956-8
[22] Brillouin, Léon. Wave propagation and group velocity. Academic Press Inc., New York (1960).
[23] C. R. Paul, Analysis of Multi conductor Transmission Lines. John Wiley & Sons., New York (1994).
[24] A. A. Fadda, A. El-Mekabaty, I. A. Mousa, K. M. Elattar, Chemistry of 3-(1*H*-Indol-3-yl)-3-oxopropanenitrile. Synthetic Communications, 2014, 44(11), 1579–1599. https://doi.org/10.1080/00397911.2013.861915
[25] N. Radwan, E. Darwish, A. Abdellatif, Synthesis, Docking and Cytotoxicity Evaluation of 3-indolyl heterocycles as Potential Anti-Cancer Agents. *Egyptian Journal of Chemistry*, 2025; 68(8): 227-239. https://doi.org/10.21608/ejchem.2024.335435.10777